Investigation of the Dynamic Characteristics of a Piezohydraulic Actuator

JAYANT SIROHI,* CHRISTOPHER CADOU AND INDERJIT CHOPRA

Alfred Gessow Rotorcraft Center, Department of Aerospace Engineering
University of Maryland, College Park, MD 20742, USA

ABSTRACT: A piezohydraulic actuator is a hybrid device consisting of a hydraulic pump driven by piezo stacks, that is coupled to a conventional hydraulic cylinder via a set of fast-acting valves. Because the performance of the actuator is strongly related to the pumping frequency, a good understanding of the dynamics of the system is essential for designing a high-efficiency actuator. This article describes the development of a frequency domain model to quantify the dynamics of a piezohydraulic hybrid actuator. The analysis treats the hydraulic circuit as a series of fluid transmission lines, each represented by a transfer matrix that determines the relationship between the pressure and velocity at the inlet and at the outlet. The model includes the effects of fluid compressibility, inertia and viscosity. An experimental procedure to measure the frequency response of the device is described, and is used to validate the analysis. The effect of tubing length and fluid viscosity on the dynamic characteristics of the system is investigated. Longer tubing lengths result in lower resonant frequencies of the system, while increasing fluid viscosity results in a decrease in the magnitude of the resonant peak.

Key Words: piezohydraulic actuator, compact hybrid actuator, hydraulic circuit frequency response, transfer matrix

INTRODUCTION

In recent years, there has been considerable interest in piezohydraulic hybrid actuators. These devices are based on the principle of frequency rectification, and combine the high energy density of piezo stacks with the versatility of fluid power transmission. The device consists of a hydraulic pump driven by piezoelectric stacks acting in conjunction with a conventional hydraulic cylinder and a fast acting set of valves. The pump pressurizes the fluid that is then utilized to transmit the power to the output hydraulic cylinder. The pump–valve–cylinder system converts the high frequency, low amplitude motion of the piezo stack to low frequency but high displacement motion of the hydraulic cylinder.

Several prototype piezohydraulic actuators have been designed and constructed over the past few years (Konishi et al., 1993, 1994; Mauck and Lynch, 2000; Nasser et al., 2000). A hybrid hydraulic actuator based on an SMA bubble actuator has also been developed (Shin et al., 2003), that has the same fundamental operational principle as a piezohydraulic actuator. Most of these research efforts described devices that operate at relatively low pumping frequencies. In previous works (Sirohi and Chopra, 2002a, 2003a), the authors described the development of a piezoelectric-hydraulic hybrid actuator as a potential actuator for a trailing edge flap on a smart rotor system. This device was tested up to a pumping frequency of 1 kHz, achieving a blocked force of 35 lb (15.75 kg) and a no-load output velocity of 1.2 in./s (30.48 mm/s). A recent prototype (Sirohi and Chopra, 2002b, 2003b) achieved a blocked force of 18 lb (8.1 kg) and a no-load velocity of approximately 3 in./s (76.2 mm/s). However, the maximum fluid flow rate in this prototype was measured at a pumping frequency of 300 Hz. At higher pumping frequencies, significant losses in flow rate were observed. Testing of this device revealed a highly nonlinear variation of the output velocity with pumping frequency.

While the research efforts described above have established the viability of the hybrid actuation concept, the power density achievable from such devices still remains far below that of the conventional electromagnetic actuators. While it is theoretically possible to surpass the power density of electromagnetic actuators by operating the hybrid devices at pumping frequencies greater than 2 kHz, a major challenge is the nonlinear behavior of fluid flow rate with pumping frequency. In order to improve the performance of these devices, accurate modeling of the behavior of the device as a function of pumping frequency is essential.

Theoretical modeling of the coupled structural-hydraulic dynamics of the actuator is complex. Several

*Author to whom correspondence should be addressed.
E-mail: sirohij@eng.umd.edu

1045-389X/05/06 0481–12 $10.00/0 DOI: 10.1177/1045389X05051072

researchers have presented models for the performance of the actuator. Nasser and Leo (2000) developed a lumped parameter model of the system converting it to an analogous mass–spring–damper system. In this model, the system is treated as two different parts, depending on each half cycle of actuation. An evaluation of the efficiency of piezopneumatic and piezohydraulic actuation was also performed using simple models. Mauck et al. (2001) developed a state-space model in which the entire system could be solved simultaneously in the time domain, however, fluid inertia was not included in the model. Konishi et al. (1997, 1998) and Regelbrugge and Anderson (2001) developed time domain solutions to directly solve the governing differential equations of the system. However, these approaches used a simplified viscous model that was validated only at one frequency, i.e., at 300 Hz. Chadou and Zhang (2003) developed a quasi-static model including the effects of output load inertia, as well as a refined viscous model for impulsively started flow. However, as the model is quasi-static, correlation with experimental data breaks down at frequencies above 400 Hz. Tang et al. (1995) developed a frequency domain model of a piezoelectrically driven hydraulic amplification device for vibration control. However, this model did not include the effects of viscosity. Simple fluid models have also been developed to predict the performance of fluid micropumps by Ullmann et al. (2001) and other researchers.

Most of the above models are based on a lumped-parameter approach, with steady-state approximations for the effect of fluid viscosity, and consequently, do not represent the system accurately at high pumping frequencies. The present work attempts to refine the above efforts by including the effects of fluid inertia and an improved model of fluid viscosity pertinent to the pumping application. A transfer matrix-type approach is adopted, with each fluid line treated as a transmission line and represented by a transfer matrix. This approach makes it easy to add additional fluid elements to the system, and to change the properties of specific elements. The fluid equations are then coupled with the structural elements and the entire system is solved in the frequency domain up to a pumping frequency of 1 kHz. The distributed parameter formulation enables accurate representation of an infinite number of modes of the system. A description of the development of the model, as well as correlation of the model with experimental data is described in this article.

DESCRIPTION OF THE PIEZOHYDRAULIC HYBRID ACTUATOR

The design and testing of piezohydraulic hybrid actuators have been described in detail by the authors in previous papers (Sirohi and Chopra, 2002b, 2003a). The goal of these early laboratory prototypes was to explore the effects of various experimental parameters on the performance of the piezoelectric pump. While there was no emphasis on compactness or system integration, consistent operation at pumping frequencies of up to 1 kHz was achieved. Recently, an improved prototype was developed. In this device, the piezoelectric pump is coupled to a conventional hydraulic cylinder by means of a manifold. Tubing of different lengths can be installed in the manifold between the pump and the output cylinder. The manifold also houses an accumulator to maintain a bias pressure on the hydraulic circuit. This results in a compact, self-contained device, that can be tested under conditions that simulate practical actuator applications.

The tested device has an output blocked force of 16 lb, with a maximum unloaded velocity of 5.5 in./s. A schematic of the actuator is shown in Figure 1(a). The solenoid valves A and B provide a bidirectional output capability and can also be incorporated in the manifold. A picture of the assembled actuator, without the solenoid valves, and without any tubing, is shown in Figure 1(b).

Piezoelectric Pump

An exploded view of the piezopump is shown in Figure 2. The pump has an outer diameter of 1.25 in., a length of 4 in. and weighs 300 g. The main components of the pump are the piezo stack assembly, piston assembly, pump body, and pumping head. The pump is actuated by two commercially available low-voltage piezo stacks (model P-804.10, TPI (1997)), bonded together end to end, with a total length of 36 mm. The piston–diaphragm assembly consists of a 1 in. diameter steel piston, clamped to a 0.002 in. thick C-1095 spring steel diaphragm. The piston has a close running fit with a bore in the pump body. One face of the pumping chamber is formed by the movable piston, the other face is formed by the pumping head that contains two passive check valves. The pumping head is mounted on the manifold using O-ring face seals.

For the present set of experiments, the check valve assembly was replaced by a steel plate with one hole, in such a way that one port was blocked by the plate while the other port was aligned with the hole. As a result, one valve was permanently closed and the other valve was permanently open, effectively eliminating the flow rectification. A sinusoidal input voltage to the piezo stacks results in a sinusoidal displacement at the output cylinder, making it very convenient to measure the frequency response of the device.

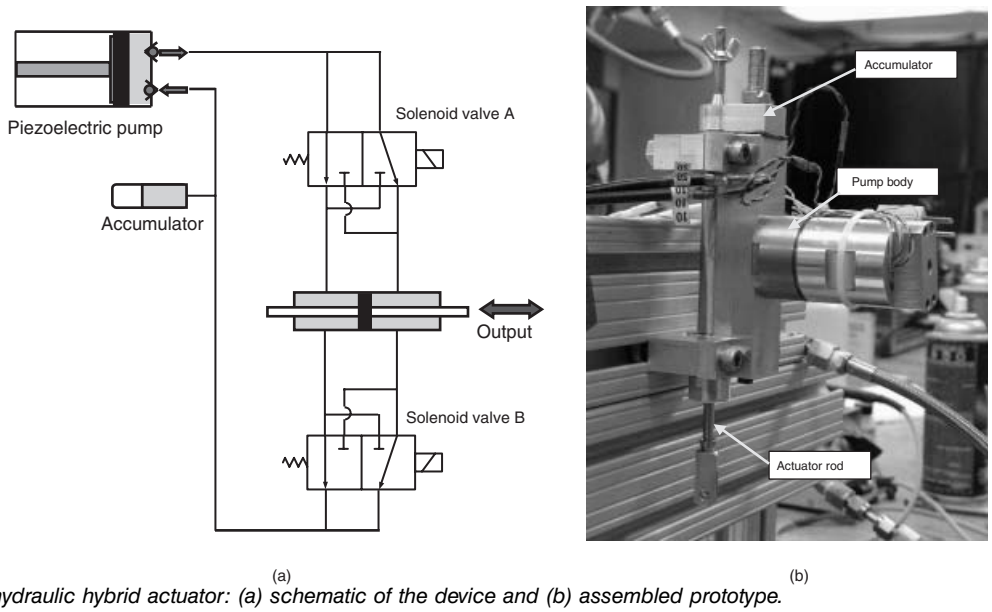

Figure 1. *Piezohydraulic hybrid actuator: (a) schematic of the device and (b) assembled prototype.*

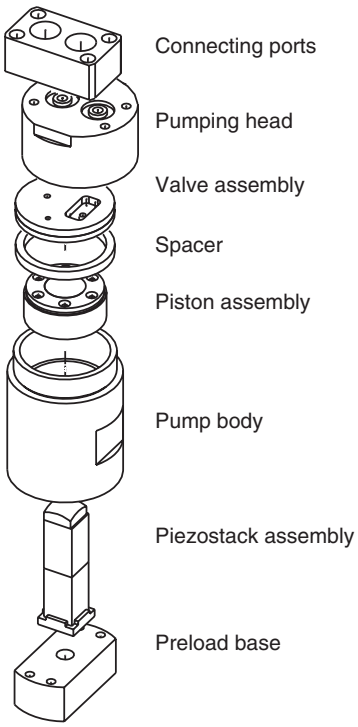

Figure 2. *Exploded view of the piezoelectric pump.*

Hydraulic Circuit

The pump is coupled to a commercially available hydraulic cylinder, with a bore of 7/16 in. and a shaft diameter of 3/16 in. by means of a manifold, designed and fabricated in-house. An accumulator is incorporated in the manifold and is used to fill fluid in the actuator as well as to maintain a bias pressure on the fluid (Figure 1(b)). It should be pointed out that the process of filling hydraulic fluid in the circuit is very important to the success of the experiment. Even a small amount of air entrained in the hydraulic circuit can drastically affect its behavior. Before filling the hydraulic fluid, all the air in the circuit is evacuated. The fluid is then introduced in the hydraulic circuit, and the accumulator is bolted on to the manifold. The accumulator is then charged with a bias pressure of 300 psi.

A list of all the important parameters of the current design is shown in Table 1. The piezo stack data, shown for each piezo stack, are taken from Lee and Chopra (2001).

From the results of earlier studies (Sirohi and Chopra, 2002b, 2003c), it was concluded that the most significant parameters affecting the response of the actuator are the bias pressure and the length of the tubing between the piezoelectric pump and the output cylinder. Therefore, in the present set of experiments, the bias pressure is kept constant, and different lengths of tubing are installed between the pump and the manifold to which the output cylinder is mounted. Standard 1/8 in. outer diameter tubing was used, with a wall thickness of 0.028 in. Tubing lengths of 0 in. (corresponding to the pump mounted directly on the output manifold, as in Figure 1(b)), 4.5 in. and 11.5 in. were installed in the hydraulic circuit, and the frequency response of each configuration was measured.

ANALYTICAL MODEL

The entire piezohydraulic actuator is divided into sections, as in Figure 3. A mathematical model for

each section of the fluid circuit is developed in terms of transfer matrices. These are subsequently combined with models for the valves, pump diaphragm, and piezo stack to yield an overall model for the hybrid system that relates the mechanical output (displacement) of the output cylinder to the electrical input to the piezo stack. The advantage of this approach is that any additional elements in the hydraulic circuit can be easily added on without affecting the rest of the formulation. It is assumed that in the frequency range of interest, up to 1 kHz, the check valves do not affect the overall response of the device. Previous experiments (Sirohi and Chopra, 2002b) indicated that the output shaft velocity was relatively insensitive to variations in the check valve resonant frequency in this range. The rectification effect of the check valves is neglected in the model, resulting in a sinusoidal displacement of the output shaft in response to a sinusoidal voltage applied to the piezo stack. The analytical model is formulated in the frequency domain, and it is expected that the variation of the output shaft velocity with the pumping frequency is the same as the variation of output shaft displacement with frequency, without flow rectification.

Table 1. Prototype device parameters.

Piezo Stack – Model P-804.10	
Number of piezo stacks	2
Length	0.3937 in.
Width	0.3937 in.
Height	0.7087 in.
Blocked force (0–100 V)	1133 lb
Free displacement (0–100 V)	≈0.5 mil
Maximum voltage	120 V
Minimum voltage	−24 V
Capacitance	≈7 μF
Hydraulic fluid – MIL-H-5606F	
Density	859 g/cc
Kinematic viscosity	15 cSt
Reference bulk modulus β_{ref}	260,000 psi
Pumping chamber	
Diameter	1 in.
Height	0.050 in.
Output actuator – double rod	
Bore diameter	0.4375 in.
Shaft diameter	0.1875 in.
Stroke	2 in.

Fluid Transfer Matrix Model

Consider a fluid in a tube, as shown in Figure 4, with the pressure (P) and volumetric flow rate (Q) quantities at each end defined by P_1, Q_1 and P_2, Q_2, respectively. An accurate model of such a fluid transmission line is developed by treating it as a distributed parameter system (Wylie and Streeter, 1978; Watton, 1989). Some basic elements of fluid transmission line theory are summarized here in order to illustrate their application in the coupled fluid-structural model of the piezohydraulic actuator.

Starting from the basic fluid equations of continuity, momentum, and energy, the relation between the pressure and flow rate variables at the ends of the fluid line can be derived in terms of a transfer matrix as:

$$\begin{Bmatrix} P_2 \\ Q_2 \end{Bmatrix} = \mathbf{T}_{12} \begin{Bmatrix} P_1 \\ Q_1 \end{Bmatrix} \tag{1}$$

where

$$\mathbf{T}_{12} = \begin{bmatrix} \cosh\Gamma & -Z_c \sinh\Gamma \\ -\dfrac{1}{Z_c}\sinh\Gamma & \cosh\Gamma \end{bmatrix} \begin{Bmatrix} P_1 \\ Q_1 \end{Bmatrix} \tag{2}$$

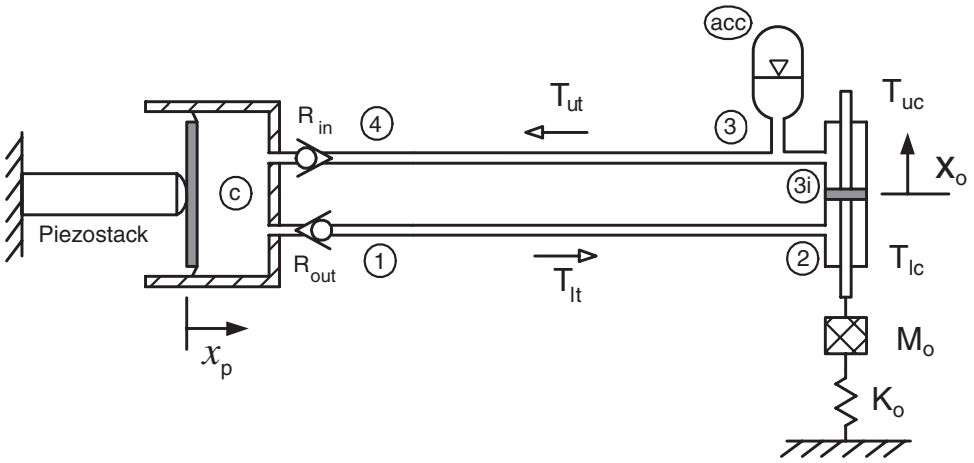

Figure 3. *Schematic of the piezohydraulic actuator system.*

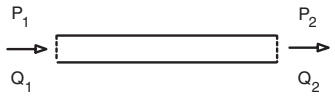

Figure 4. *Schematic of the flow through a section of tubing.*

This is a standard representation used in hydraulic analyses, however, it is worth noting the following assumptions that are inherent in this method:

1. fluid velocity is much smaller than the acoustic velocity
2. laminar fluid flow in a rigid tube of circular cross section
3. length of the tube is much larger than its diameter ($l/r \gg 1$)
4. normalized density variations are small ($\Delta\rho/\rho \ll 1$)

The behavior of the fluid line is governed by two quantities; the characteristic impedance Z_c and the propagation parameter Γ. For an inviscid fluid, these quantities are given by

$$\Gamma = \bar{D}_c = \frac{1}{\omega_c}\frac{d}{dt} \tag{3}$$

$$Z_c = Z_o = \frac{\rho c_o}{\pi r^2} \tag{4}$$

where $\omega_c = c_o/l$ is the characteristic frequency of the fluid line, and the speed of sound in the fluid, c_o is given by

$$c_o = \sqrt{\frac{\beta}{\rho}} \tag{5}$$

Fluid viscosity can be incorporated in two ways: one could use a linear friction model using a friction factor calculated from Hagen–Poiseuille flow theory, or a dissipative model derived using the energy equation (Goodson and Leonard, 1972). This results in different expressions for Γ and Z_c compared to the inviscid case, while the basic transfer matrix (Equation (1)) between pressure and flow quantities remains the same. The exact solution for liquids with frequency-dependent viscous dissipation yields expressions for Γ and Z_c in terms of a ratio of Bessel functions, B_r as given here (Iberall, 1950; Rohmann and Gorgan, 1957; Brown, 1962; Nicholas, 1962)

$$\Gamma = \bar{D}_c\left[\frac{1}{1-B_r}\right]^{1/2} \tag{6}$$

$$Z_c = Z_o\left[\frac{1}{1-B_r}\right]^{1/2} \tag{7}$$

where

$$B_r = \frac{2J_1(j\sqrt{8\bar{D}_v})}{j\sqrt{8\bar{D}_v}J_0(j\sqrt{8\bar{D}_v})} \tag{8}$$

In the above equation, J_0 and J_1 are ordinary Bessel functions of the first kind. The operator $\bar{D}_v$ is defined in terms of the viscous frequency, ω_v by

$$\bar{D}_v = \frac{1}{\omega_v}\frac{d}{dt} \tag{9}$$

where

$$\omega_v = \frac{8\nu}{d^2} \tag{10}$$

Equations (2)–(10) constitute a comprehensive model of the fluid lines, incorporating the effects of fluid inertia, compressibility as well as viscous dissipation.

Frequency Response of the Device

The frequency response of the device is calculated by assuming a harmonic excitation at a frequency ω, resulting in the following substitution for the operator D

$$D = j\omega \tag{11}$$

This substitution greatly simplifies the fluid line Equations (2)–(10). The Bessel function ratio, B_r, can be expressed as either an infinite product, a simple series sum, or a partial fraction expansion. However, in order to accurately represent this ratio, especially at high frequencies, a large number of terms are required. While several approximations to the Bessel function ratios or to Γ and Z_c have been investigated in the past (Brown, 1962, 1969; Nichols, 1962; Oldenburger and Goodson, 1964; Karam and Franke, 1967; Goodson and Leonard, 1972; Woods, 1983), a first-order square root approximation (Woods, 1983) was chosen for the present calculations because of its simplicity, as well as its accuracy over both high and low frequency ranges. This approximation is given by

$$B_r = \frac{1}{\sqrt{1+2\bar{D}_v}} \tag{12}$$

The fluid model with the above simplifications can now be easily incorporated into the complete system model. The equations governing the behavior of the other components of the piezohydraulic actuator are described here. Force equilibrium on the piezo stack gives:

$$c_v V - P_c a_p = m_p\ddot{x}_p + b_p\dot{x}_p + k_p x_p \tag{13}$$

The continuity equation for the pumping chamber can be written as:

$$C_c\dot{P}_c = a_p\dot{x}_p + Q_4 - Q_1 \tag{14}$$

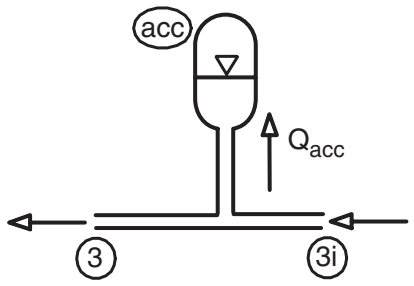

Figure 5. *Schematic of the accumulator.*

where the fluid capacitance of the pumping chamber, C_c, is given by McCloy and Martin (1980), Watton (1989)

$$C_c = \frac{a_p \Delta_{gap}}{\beta} \tag{15}$$

The accumulator can be treated as a section of tubing with a local compliance much higher than the surrounding fluid. Such an approximation results in a constant pressure across the accumulator, and a difference in the flow rate upstream and downstream of the accumulator. This can be seen more clearly in Figure 5, where the difference between upstream and downstream flow rates enters the accumulator. Because the accumulator is assumed to have a local effect,

$$P_{3i} = P_3 = P_{acc} \tag{16}$$

Flow continuity between stations '3' and '3*i*' requires that

$$Q_3 = Q_{3i} + Q_{acc} \tag{17}$$

where Q_{acc} is the flow entering the accumulator. This flow results in a change in the accumulator pressure given by

$$C_{acc}\dot{P}_{acc} = Q_{acc} \tag{18}$$

where C_{acc} is the fluid capacitance of the accumulator, given by Equation (15), with the corresponding values of the variables for the accumulator. From Equations (16)–(18), the point transfer matrix (Wylie and Streeter, 1978) between stations '3' and '3*i*' can be written as:

$$\begin{Bmatrix} P_3 \\ Q_3 \end{Bmatrix} = \mathbf{T}_{acc} \begin{Bmatrix} P_{3i} \\ Q_{3i} \end{Bmatrix} \tag{19}$$

$$= \begin{bmatrix} 1 & 0 \\ -sC_{acc} & 1 \end{bmatrix} \begin{Bmatrix} P_{3i} \\ Q_{3i} \end{Bmatrix} \tag{20}$$

Assuming the output mechanical load to be lumped together with the output piston, force equilibrium on the output piston gives

$$(P_{lp} - P_{up})a_o = m_o\ddot{x}_o + b_o\dot{x}_o + k_o x_o \tag{21}$$

From the geometry of the output cylinder, it can be seen that

$$Q_{up} = Q_{lp} = a_o\dot{x}_o \tag{22}$$

At the check valves,

$$P_c - P_1 = R_{out}Q_1 \tag{23}$$

$$P_4 - P_c = R_{in}Q_4 \tag{24}$$

where the values of R_{out} and R_{in} determine the dependence of the flow through the check valves on the differential pressure across them.

From Equations (1)–(21),

$$\begin{Bmatrix} P_1 \\ Q_1 \end{Bmatrix} = \mathbf{A} \begin{Bmatrix} P_{lp} \\ a_o\dot{x}_o \end{Bmatrix} \tag{25}$$

(26)

$$\begin{Bmatrix} P_4 \\ Q_4 \end{Bmatrix} = \mathbf{B} \begin{Bmatrix} P_{up} \\ a_o\dot{x}_o \end{Bmatrix} \tag{27}$$

where the matrices **A** and **B** are given by

$$\boldsymbol{A} = (\mathbf{T}_{lt} \cdot \mathbf{T}_{lc})^{-1} = \begin{bmatrix} A_{11} & A_{12} \\ A_{21} & A_{22} \end{bmatrix} \tag{28}$$

$$\boldsymbol{B} = \mathbf{T}_{ut} \cdot \mathbf{T}_{acc} \cdot \mathbf{T}_{uc} = \begin{bmatrix} B_{11} & B_{12} \\ B_{21} & B_{22} \end{bmatrix} \tag{29}$$

The above equations can be simplified as:

$$\mathbf{M}\{\ddot{q}\} + \mathbf{C}\{\dot{q}\} + \mathbf{K}\{q\} = \{F\} \tag{30}$$

where the vector $\{q\}$ contains the system variables and is given by

$$\{q\} = \begin{Bmatrix} x_p \\ x_o \\ P_c \\ P_1 \\ P_4 \\ P_{lp} \\ P_{up} \end{Bmatrix} \tag{31}$$

The coefficient matrices **M**, **C**, and **K** are given by

$$\mathbf{M} = \begin{Bmatrix} m_p & 0 & 0 & 0 & 0 & 0 & 0 \\ 0 & m_o & 0 & 0 & 0 & 0 & 0 \\ 0 & 0 & 0 & 0 & 0 & 0 & 0 \\ 0 & 0 & 0 & 0 & 0 & 0 & 0 \\ 0 & 0 & 0 & 0 & 0 & 0 & 0 \\ 0 & 0 & 0 & 0 & 0 & 0 & 0 \\ 0 & 0 & 0 & 0 & 0 & 0 & 0 \end{Bmatrix} \tag{32}$$

$$\mathbf{C} = \begin{Bmatrix} b_p & 0 & 0 & 0 & 0 & 0 & 0 \\ 0 & b_o & 0 & 0 & 0 & 0 & 0 \\ 0 & R_{out}A_{22}a_o & 0 & 0 & 0 & 0 & 0 \\ 0 & A_{12}a_o & 0 & 0 & 0 & 0 & 0 \\ 0 & B_{12}a_o & 0 & 0 & 0 & 0 & 0 \\ 0 & R_{in}B_{22}a_o & 0 & 0 & 0 & 0 & 0 \\ -a_p & 0 & C_c & 0 & 0 & 0 & 0 \end{Bmatrix} \quad (33)$$

$$\mathbf{K} = \begin{Bmatrix} k_p & 0 & a_p & 0 & 0 & 0 & 0 \\ 0 & k_o & 0 & 0 & 0 & -a_o & a_o \\ 0 & 0 & -1 & 1 & 0 & R_{out}A_{21} & 0 \\ 0 & 0 & 0 & -1 & 0 & A_{11} & 0 \\ 0 & 0 & 0 & 0 & -1 & 0 & B_{11} \\ 0 & 0 & 1 & 0 & -1 & 0 & R_{in}B_{21} \\ 0 & 0 & \dfrac{1}{R_{in}}+\dfrac{1}{R_{out}} & -\dfrac{1}{R_{out}} & -\dfrac{1}{R_{in}} & 0 & 0 \end{Bmatrix} \quad (34)$$

The forcing on the system is given by the vector $\{F\}$

$$\{F\} = \begin{Bmatrix} c_v V \\ 0 \\ 0 \\ 0 \\ 0 \\ 0 \\ 0 \end{Bmatrix} \quad (35)$$

For harmonic forcing at a frequency ω, the solution to the above system of equations can be written as:

$$\{q\} = (-\omega^2\mathbf{M} + j\omega\mathbf{C} + \mathbf{K})^{-1}\{F\} \quad (36)$$

For a time domain simulation, the check valve resistances are dependent on the differential pressure across them, which is given by the system variables P_c, P_1, and P_4. However, in the present frequency response analysis, constant values of R_{out} and R_{in} are assumed. By setting $R_{in} = \infty$ and $R_{out} = 0$, one valve is permanently closed and the other permanently open. This represents the dynamics of the real device with check valves during one half of the pumping cycle, the other half being symmetric.

Equation (36) is solved to obtain the frequency response of the system variables in the vector $\{q\}$. Because the hyperbolic sines and cosines are calculated exactly, the calculated frequency response accurately represents an infinite number of modes, which is a significant advantage over typical lumped parameter methods. The response of the system is calculated up to pumping frequencies of 1 kHz for correlation with experiments. It should be noted that the above analysis assumes a constant bulk modulus of the fluid, whereas in reality it depends on the pressure in the fluid. However, for a preliminary analysis in order to identify which parameters of the device have a dominant effect on its frequency response, this effect can be neglected.

EXPERIMENTAL SETUP

A schematic of the experimental setup is shown in Figure 6. It can be seen that one of the check valves is permanently closed and the other one is permanently open. The output displacement is measured by a laser vibrometer. As a result of the elimination of the check valves, a sinusoidal voltage applied to the piezo stacks results in a sinusoidal output displacement. For simplicity, the entire piezohydraulic system is assumed to be linear.

A swept sine, from a frequency of 50 Hz to 1 kHz is input to a power amplifier, which actuates the piezo stacks. The actuating waveform is offset by a DC value equal to the amplitude of the sinusoid. This ensures that the piezo stacks are only actuated by a positive voltage, and minimizes the possibility of piezo stack failure due to tensile stresses. At each frequency of actuation, the magnitude and phase of the displacement of the output shaft are measured. While the actual device can be actuated with voltages from 0 to 100 V, the voltage amplitude for the present testing was conducted at 12.5 and 25 V, due to amplifier current limitations.

The entire device is bolted onto a vibration isolation table, as shown in Figure 7. The output shaft displacement was measured by a laser displacement sensor and a laser vibrometer. The displacement of the output shaft is on the order of a few microns, and it was observed that the signal to noise ratio of the laser displacement sensor was not sufficiently high for accuracy of the data. Therefore, all the measurements reported in this paper were taken with the laser vibrometer. It should be noted that the output of the laser vibrometer is proportional to the velocity of the output shaft. However, as we have assumed a linear system, the displacement of the output shaft is obtained from

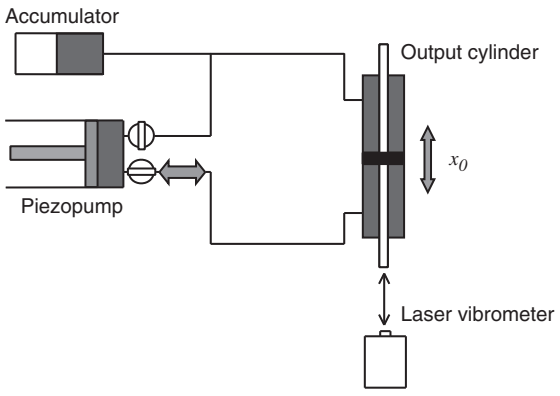

Figure 6. *Schematic of the test setup.*

the laser vibrometer measurements simply by dividing the velocity measurements by $j\omega$, where ω is the frequency of actuation in rad/s.

RESULTS AND DISCUSSION

With the frequency domain analysis, it is possible to investigate the effect of various system parameters on the frequency response of the device. The bulk modulus and density of the hydraulic fluid have a significant effect on the frequency response of the system. However, since most hydraulic fluids have similar values of bulk modulus and density, only the effects of fluid viscosity and tubing length are investigated in this study. The analytical results for the response with different tubing lengths is correlated with experimental measurements. Because the effect of viscosity was not very large for fluid viscosity in the range of 2–20 cSt, experiments were performed with only one hydraulic fluid, with a viscosity of 2 cSt.

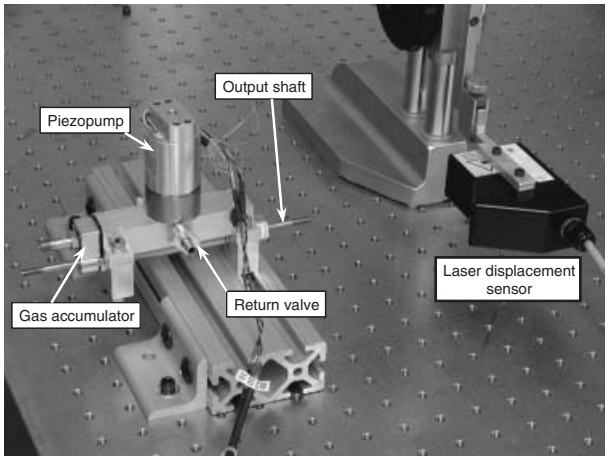

Figure 7. *Measurement of the displacement of the output shaft.*

Analytical Predictions

The effect of the length of the fluid line on the frequency response of the system variables x_o and P_c, for a fluid of kinematic viscosity $\nu = 2$ cSt is shown in Figure 8. It can be seen that a large increase in output displacement is obtained at the resonant condition, and that the resonant frequency is strongly dependent on the length of the fluid line. A large increase in the pumping chamber pressure is also observed, resulting in maximum pressures of ≈2800 psi. It should be noted that the present analysis assumes that the pump body is infinitely rigid, however, in reality the finite compliance of the pump body results in considerably lower pressures.

Figure 9 shows the dependence of the frequency response of the system variables x_o and P_c on the fluid viscosity, for a fluid line length of 4.5 in. As expected, it can be seen that the effect of viscosity is similar to an increase in viscous damping of the system. It can be seen that the effect of changing the viscosity from 2 to 20 cSt is relatively small compared to the effect of changing it from 20 to 200 cSt.

From the above results, it can be concluded that the frequency response is dominated by the dynamics of the hydraulic circuit, and this offers a powerful method of increasing the output power of the device. While similar concepts have been investigated in the past (Suzuki, 1987; Konishi et al., 1994) the present 'exact' analysis enables a more accurate prediction of the device behavior that includes the effects of fluid viscosity.

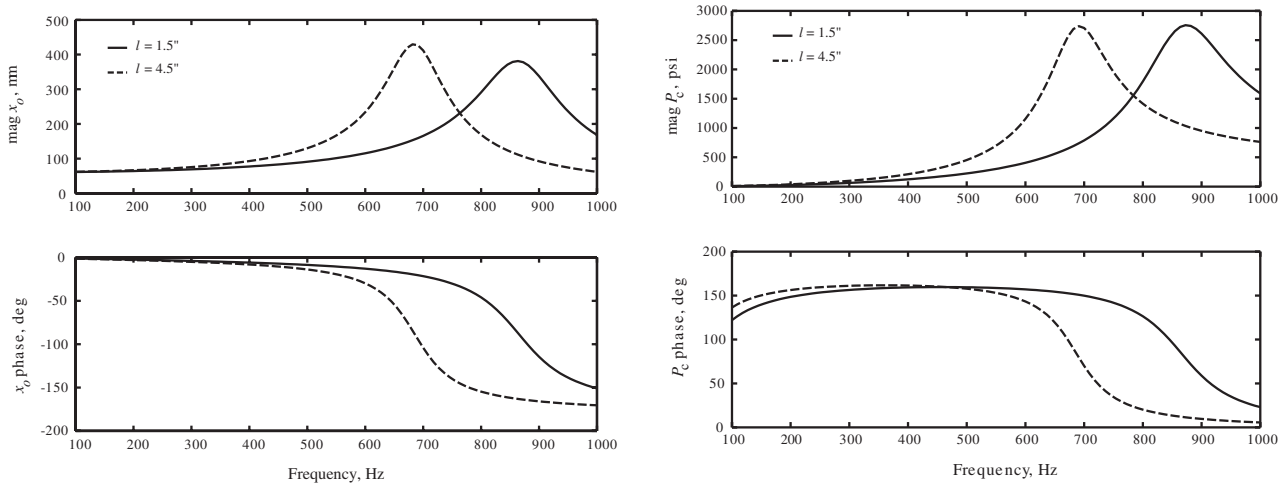

Figure 8. *Theoretical variation of output displacement x_0 and pumping chamber pressure P_c with tubing length, $v = 2$ cSt.*

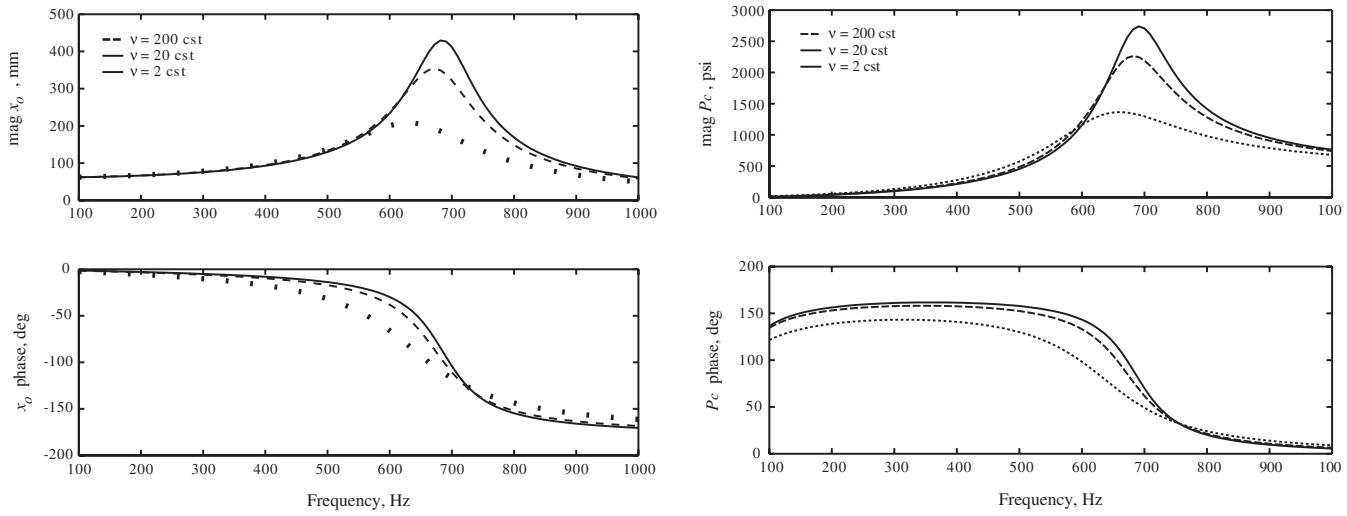

Figure 9. *Theoretical variation of piston output displacement x_0 and pumping chamber pressure P_c with fluid viscosity, length, l=4.5 in.*

Correlation with Experimental Data

Figure 10 shows a comparison of the predicted and measured frequency response functions of the output displacement, for tubing lengths of 0, 4.5, and 11.5 in. In general, it can be seen that the analysis underpredicts the first natural frequency by 10–15%. Below the resonant peak, the magnitude of the response is predicted well. However, at frequencies higher than the resonance, there is a significant underprediction of the response. Regarding the phase of the response, there is an underprediction (10–30°) below resonance and a mixed variation above the resonance condition. Another important observation that can be made from Figure 10(c) is the presence of a secondary peak in the measured response, at ≈600 Hz. This peak is not captured by the analysis, and may arise from the compliance of the structure or wave reflections from various internal components in the device.

Measured Nonlinearities

In order to investigate the causes of the discrepancy between analysis and experiment, it is useful to look closely at the time domain signal from the vibrometer, which is directly proportional to the velocity of the output shaft. Based on the assumptions regarding the linear behavior of the system, a purely sinusoidal waveform is expected. Figure 11 shows the signal from the vibrometer at pumping frequencies of 100 and 600 Hz, at an actuation voltage of amplitude 25 V. Although the driving voltage is sinusoidal, it can be clearly seen that the output waveforms are not purely sinusoidal. The most notable feature is the presence of a discontinuous region around each zero crossing, with a lower slope than the neighboring regions. Because the scaled voltage signal is proportional to velocity, the zero crossing region corresponds to the time period around which the output shaft achieves its maximum displacement. At this time, the output shaft changes direction and momentarily achieves zero velocity. As a result, we attribute this discontinuous region to static friction in the rod seals around the output shaft. Since this region occupies a considerable fraction of the total time period, frictional effects may also be very important.

Another consequence of the assumption of a linear system is that the transfer function between the input voltage and output displacement should be independent of the magnitude of the input voltage. In order to verify the accuracy of this assumption, the frequency response of the output displacement was measured as described above at actuation voltages of amplitude 12.5 and 25 V. Figure 12 shows the comparison between the two frequency response functions. It can be seen that at the higher actuation voltage of 25 V, the first resonant peak moves to a lower frequency compared to the case of the 12.5 V actuation voltage.

This shows that the assumption of linearity in the actuator system is an approximation, and explains, at least in part, the discrepancy between the analytical predictions and experimental results.

CONCLUSIONS

The power density of a piezohydraulic actuator can be increased by operating it at higher pumping frequencies, however, a good understanding of the

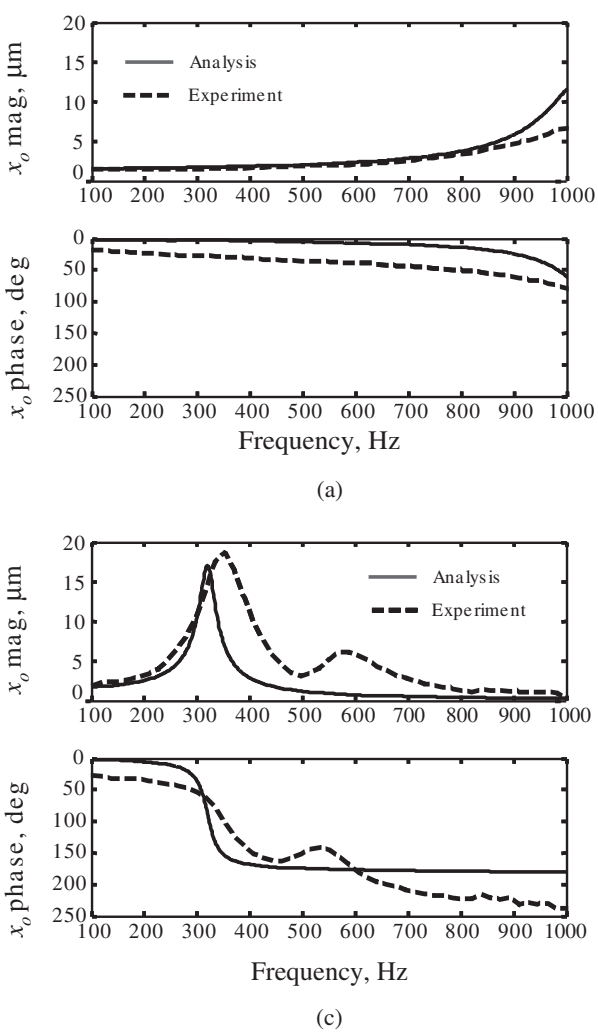

Figure 10. *Comparison of experimental an analytical frequency response functions: (a) no tubes, pump directly attached to manifold; (b) tubing length = 4.5 in.; and (c) tubing length = 11.5 in.*

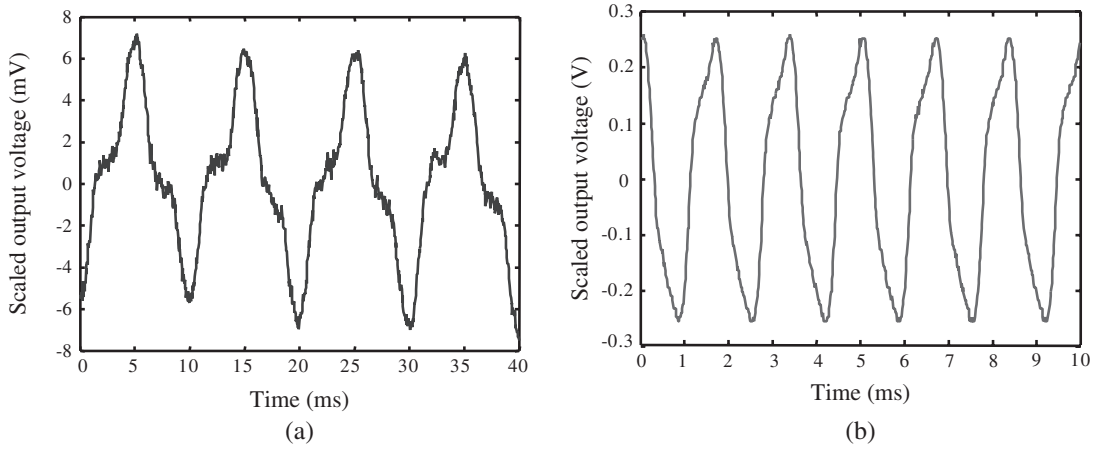

Figure 11. *Vibrometer output signal in the time domain, actuation voltage amplitude 25 V: (a) pumping frequency 100 Hz and (b) pumping frequency 600 Hz.*

dynamics of the device is necessary for optimum design. This article describes the development of a frequency domain model for the dynamic behavior of a piezo-hydraulic actuator using transmission line theory. The analysis was used to investigate the effects of tubing length and fluid viscosity on the performance of the device. The effect of increasing tubing length is to reduce the resonant frequency of the system. Fluid viscosity

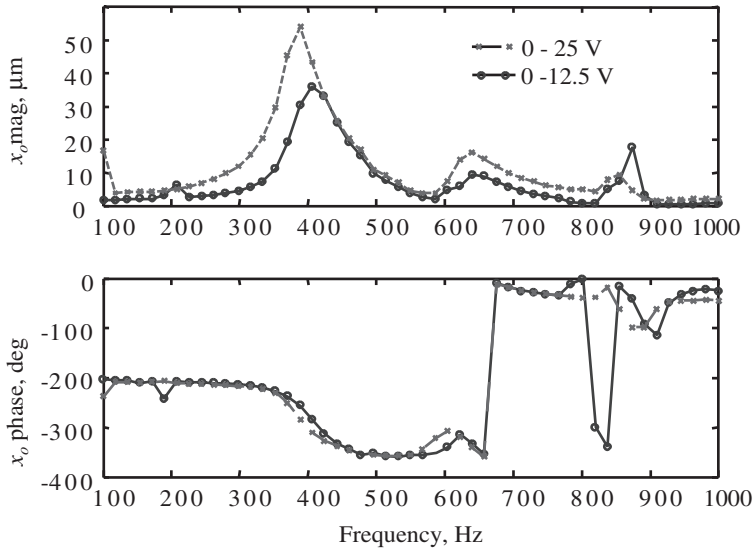

Figure 12. *Effect of actuation voltage on the frequency response function.*

affects the system in a manner similar to viscous damping.

The analysis was validated by experiments performed on a prototype piezohydraulic actuator. The flow rectification was eliminated by removing the check valves on the pump. The transfer function between output displacement and piezostack driving voltage was measured using a laser vibrometer. It was observed that overall, the analysis correlates well with the measured results for frequencies below the first natural frequency of the system. Given the dimensions of the system, the natural frequency can be predicted with an accuracy of 10–15%. While a better accuracy may be desirable to properly understand the dynamics of the actuator, the present analysis appears sufficient for the preliminary design of an actuator.

Discrepancies between theory and analysis may be due to significant nonlinearities in the system, such as static friction in the rod seals. This was observed as a distortion in the time domain output displacement signal. In addition, it was observed that the magnitude of output displacement was not linearly dependent on the magnitude of the piezo stack driving voltage. In future modeling efforts, the nonlinearities such as static friction in the rod seals, and dependence of the frequency response on the magnitude of actuation voltage will need to be included in order to represent the system accurately.

NOMENCLATURE

System Quantities

a = area (m^2)
b = damping (NS/m)
β = fluid bulk modulus (Pa)
C = fluid capacitance (m^3/Pa)
c_0 = speed of sound (m/s)
c_v = piezo stack coefficient (N/V)
Δ_{gap} = pumping chamber height (m)
D = operator (d/dt)
$\bar{D}_c$ = operator (D/ω_c)
$\bar{D}_v$ = operator (D/ω_v)
Γ = propagation parameter (rad/s^2)
$j = \sqrt{-1}$
k = stiffness (N/m)
l = length of fluid line (m)
m = mass (kg)
v = kinematic viscosity (m^2/s)
P = pressure (Pa)
Q = volumetric flow rate (m^3/s)
ρ = density (kg/m^3)
r = radius of fluid line (m)
R = fluid resistance (Pa s/m^3)
s = laplace variable (1/s)
$\mathbf{T}$ = transfer matrix
V = applied voltage (V)
ω = frequency (rad/s)
ω_c = characteristic frequency (rad/s)
ω_v = viscous frequency (rad/s)
x = displacement (m)
Z_c = characteristic impedance ($kg/m^4/s$)
Z_o = characteristic impedance, inviscid case ($kg/m^4/s$)

Subscripts

acc = accumulator
c = pumping chamber
in = 'in' check valve
lc = high pressure side of the output cylinder

lp = high pressure face of the output piston
lt = high pressure side of the tubing
o = output actuator piston
out = 'out' check valve
p = pumping chamber piston
uc = low pressure side of the output cylinder
up = low pressure face of the output piston
ut = low pressure side of the tubing

ACKNOWLEDGMENTS

The authors would like to acknowledge CSA Engineering Inc., and DARPA for their support. Useful discussions with Dr. Jinhyeong Yoo, Dr. Eric Anderson, and Jason Lindler are also gratefully acknowledged.

REFERENCES

1997. *Products for Micropositioning*, US-edition, Physik Instrumente (PI).

Brown, F.T. 1962. "The Transient Response of Fluid Lines," *Journal of Basic Engineering, Transactions of the ASME, Series D,* 84(4):547–553.

Brown, F.T. 1969. "A Quasi Method of Characteristics with Application to Fluid Lines with Frequency Dependent Wall Shear and Heat Transfer," *Journal of Basic Engineering, Transactions of the ASME.*

Cadou, C. and Zhang, B. 2003. "Performance Modeling of a Piezo-Hydraulic Actuator," *Journal of Intelligent Material Systems and Structures*, 14(3):149–160.

Goodson, R.E. and Leonard, R.G. 1972. "A Survey of Modeling Techniques for Fluid Line Transients," *Journal of Basic Engineering, Transactions of the ASME, Series D*, 94:474–482.

Iberall, A.S. 1950. "Attenuation of Oscillatory Pressures in Instrument Lines," *Journal of Research, National Bureau of Standards*, 45:2115.

Karam, J.T. and Franke, M.E. 1967. "The Frequency Response of Pneumatic Lines, Journal of Basic Engineering," *Transactions of the ASME, Series D*, 90(2):371–378.

Konishi, K., Yoshimura, T., Hashimoto, K. and Yamamoto, N. 1993. "Hydraulic Actuators Driven by Piezoelectric Elements (1st Report, Trial Piezoelectric Pump and its Maximum Power)," *Journal of Japanese Society of Mechanical Engineering (C)*, 59(564):213–220.

Konishi, K., Yoshimura, T., Hashimoto, K., Hamada, T. and Tamura, T. 1994. "Hydraulic Actuators Driven by Piezoelectric Elements (2nd Report, Enlargement of Piezoelectric Pumps Output Power Using Hydraulic Resonance)," *Journal of Japanese Society of Mechanical Engineering (C)*, 60(571):228–235.

Konishi, K., Ukida, H. and Kotani, T. 1997. "Hydraulic Actuators Driven by Piezoelectric Elements (4th report, Construction of Mathematical Models for Simulation)," *Journal of Japanese Society of Mechanical Engineering (C)*, 63(605):158–165.

Konishi, K., Ukida, H. and Sawada, K. 1998. "Hydraulic Pumps Driven by Multilayered Piezoelectric Elements – Mathematical Model and Application to Brake Device," In: *Proceedings of the 13th Korean Automatic Control Conference*.

Lee, T. and Chopra, I. 2001. "Design of Piezostack-Driven Trailing-edge Flap Actuator for Helicopter Rotors," *Smart Materials and Structures*, 10(1):15–24.

Mauck, L.D. and Lynch, C.S. 2000. "Piezoelectric Hydraulic Pump Development," *Journal of Intelligent Material Systems and Structures*, 11:758–764.

Mauck, L.D., Oates, W.S. and Lynch, C.S. 2001. "Piezoelectric Hydraulic Pump Performance," In: *Proceedings of the 8th SPIE Conference on Smart Structures and Materials: Industrial and Commercial Applications of Smart Structures Technologies*, Newport Beach, CA, Vol. 4332, pp. 246–253.

McCloy, D. and Martin, H. 1980. *Control of Fluid Power: Analysis and Design*, 2nd (revised) edn, Ellis Horwood Limited, Chichester, England.

Nasser, K. and Leo, D.J. 2000. "Efficiency of Frequency-Rectified Piezohydraulic and Piezopneumatic Actuation," *Journal of Intelligent Material Systems and Structures*, 11:798–810.

Nasser, K., Leo, D.J. and Cudney, H.H. 2000. "Compact Piezohydraulic Actuation System," In: *Proceedings of the 7th SPIE Conference on Smart Structures and Integrated Systems*, Newport Beach, CA, Vol. 3991, pp. 312–322.

Nichols, N.B. 1962. "The Linear Properties of Pneumatic Transmission Lines," *ISA Transactions*, 1(1).

Oldenburger, R. and Goodson, R.E. 1964. "Simplification of Hydraulic Line Dynamics by Use of Infinite Products," *Journal of Basic Engineering, Transactions of the ASME, Series D*, 86:1–10.

Regelbrugge, M. and Anderson, E. 2001. "Solid-Fluid Hybrid Actuation: Concepts, Models," In: *Capabilities and Limitations, Proceedings of the 12th International Conference on Adaptive Structures Technology*, College Park, MD, Vol. 20742, pp. 60–69.

Rohmann, C.P. and Grogan, E.C. 1957. "On the Dynamics of Pneumatic Transmission Lines," *Transactions of ASME*, 79:853.

Shin, D., Lee, D., Mohanchandra, K.P. and Carman, G.P. 2003. "Development of a SMA-based Actuator for Compact Kinetic Energy Missile," In: *Proceedings of the 10th SPIE Conference on Smart Structures and Integrated Systems*, San Diego, CA, Vol. 4701, pp. 237–243.

Sirohi, J. and Chopra, I. 2002a. "Design and Testing of a High Pumping Frequency Piezoelectric-hydraulic Hybrid Actuator," In: *Proceedings of the 9th SPIE Conference on Smart Structures and Integrated Systems*, San Diego, CA.

Sirohi, J. and Chopra, I. 2002b. "Design and Testing of a High Pumping Frequency Piezoelectric-hydraulic Hybrid Actuator," In: *Proceedings of the 13th International Conference on Adaptive Structures Technology,* Potsdam, Germany.

Sirohi, J. and Chopra, I. 2003a. "Design and Development of a High Pumping Frequency Piezoelectric-hydraulic Hybrid Actuator," *Journal of Intelligent Material Systems and Structures*, 14(3):135–148.

Sirohi, J. and Chopra, I. 2003b. "Measurement of the Dynamic Response of a Piezohydraulic Actuator," In: *Proceedings of the 14th International Conference on Adaptive Structures Technology*, Seoul, Korea.

Sirohi, J. and Chopra, I. 2003c. "Performance Modeling of a Piezohydraulic Actuator," In: *Proceedings of the 44th AIAA/ASME/ASCE/AHS/ASC Structures, Structural Dynamics, and Materials Conference*, Norfolk VA, AIAA Paper #2003-1641.

Suzuki, K. 1987. "A New Hydraulic Pressure Intensifier using Oil Hammer," In: *Fluid Transients in Fluid-Structure Interaction*, ASME Special Publication for the ASME Winter Annual Meeting, Boston, Massachusetts, pp. 43–50.

Tang, P., Palazzolo, A., Kascak, A., Montague, G. and Li, W. 1995. "Combined Piezoelectric-Hydraulic Actuator Based Active Vibration Control for a Rotordynamic System," *Journal of Vibration and Acoustics*, 117:285–293.

Ullmann, A., Fono, I. and Taitel, Y. 2001. "A Piezoelectric Valve-less Pump – Dynamic Model," *Transactions of the ASME*, 123:92–98.

Watton, J. (1989). *Fluid Power Systems*, Prentice Hall.

Woods, R.L. 1983. "A First-order Square Root Approximation for Fluid Transmission Lines," in *Fluid Transmission Line Dynamics*, ASME Special publication for the ASME Winter Annual Meeting, Washington, D.C., pp. 37–50.

Wylie, E.B. and Streeter, V.L. 1978. *Fluid Transients*, McGraw-Hill International Book Company.